AGU ADVANCING EARTH AND SPACE SCIENCE

Geophysical Research Letters®

RESEARCH LETTER
10.1029/2021GL096559

Key Points:

- Flexural strength of freshwater and saline ice increases upon cycling by as much as a factor of two or more
- Cyclically-induced increase in flexural strength of freshwater and saline ice is fully relaxed upon annealing
- The relaxation of the original strength is attributed to the relaxation of the cyclically-induced internal back stress

Correspondence to:

A. Murdza,
andrii.murdza@dartmouth.edu

Citation:

Murdza, A., Schulson, E. M., & Renshaw, C. E. (2022). Relaxation of flexure-induced strengthening of ice. *Geophysical Research Letters*, *49*, e2021GL096559. https://doi.org/10.1029/2021GL096559

Received 21 OCT 2021
Accepted 7 FEB 2022

Relaxation of Flexure-Induced Strengthening of Ice

A. Murdza[1], E. M. Schulson[1], and C. E. Renshaw[1,2]

[1]Thayer School of Engineering, Dartmouth College, Hanover, NH, USA, [2]Department of Earth Sciences, Dartmouth College, Hanover, NH, USA

Abstract Increasing fetch as sea ice retreats with global warming is increasing the amplitude of ocean waves, motivating the need for a better understanding of the impact of episodic flexing on the strength of ice. Unexpectedly, recent studies showed that the flexural strength of ice increases by as much as a factor of two or more upon cyclic loading (unlike earlier results where ice had a thermo-mechanical history that could account for the difference), possibly owing to the development of internal back stress originating from dislocation pileups. New systematic experiments reveal that the cyclically-induced increase in flexural strength of columnar-grained S2 freshwater and saline ice is fully relaxed upon annealing at high homologous temperatures ($T_h = 0.91$ and 0.96). Moreover, the ice can be repeatedly strengthened to the same level by cyclic loading if allowed to anneal after each episode of strengthening. The relaxation of the original strength is attributed to the relaxation of the cyclically-induced internal back stress.

Plain Language Summary Recent studies have revealed that as the ice coverage on the Arctic Ocean decreases due to global warming, the amplitude of ocean waves increases, leading to an increase of bending stresses within the ice and to the potential for subsequent failure. However, it was recently discovered that the strength of ice increases upon flexing up and down, unlike earlier results where natural sea ice potentially had many micro- and macrocracks that could account for the decrease in strength. To understand the behavior of ice under repetitive loading we conducted and describe new systematic experiments in the present study. We find that the increase in flexural strength of both freshwater and saline ice is fully relaxed if the ice is allowed to anneal (to be unloaded) for up to 48 hr. In other words, the results imply that an ice cover is the weakest and, thus, most susceptible to failure after long "quiet" periods related to the absence of ocean waves.

1. Introduction

Richter-Menge et al. (2002) observed that the mechanical behavior of the nearshore Arctic ice cover is impacted by repeated periods of both low, nearly zero, and high stresses due to shifting wind direction and magnitude. Similarly, recent studies have revealed that cyclic loading of the ice cover by oceanic waves plays a significant role in the evolution of ice extent, thickness, internal stress distribution, and mechanical behavior (Kohout et al., 2014; Meylan et al., 2014; Stopa et al., 2018; Sutherland & Dumont, 2018). Sea ice and ice shelves (Holdsworth, 1969; Sergienko, 2010; Vinogradov & Holdsworth, 1985) are subjected to episodic flexing through the action of oceanic waves whose amplitude is increasing owing to growing fetch as ice retreats during global warming (Francis et al., 2011; Thomson & Rogers, 2014). As a result, flexural stresses within the ice are also expected to increase, possibly leading to increasing flexural failure (Asplin et al., 2012; Collins et al., 2015; Kohout et al., 2016; Liu et al., 1988; Prinsenberg & Peterson, 2011), with consequent impacts on water-atmosphere heat exchange and melt rates due to the negative impact of fragmentation on ice cover albedo (Massom & Stammerjohn, 2010; Pistone et al., 2014; Steele, 1992; Zhang et al., 2019) and on coastal erosion through the impact of ocean swells that can travel deeper into the fragmented ice-covered ocean with less attenuation (Ardhuin et al., 2020; Kohout et al., 2014; Meylan et al., 2015; Toffoli et al., 2015). The crusts of Jupiter's Europa and Saturn's Enceladus and of other icy satellites which overlie putative oceans are similarly subjected to cyclic loading through tidal forces (Burns & Matthews, 1986; Hammond et al., 2018) and, as a result, also subject to flexural failure.

The behavior of ice under cyclic loading and a corresponding decrease/increase in ice strength (more below) was investigated previously (D. M. Cole, 1990; Hammond et al., 2018; Haskell et al., 1996; Iliescu et al., 2017; Langhorne et al., 1998; Murdza et al., 2020, 2021). However, nothing (to our knowledge) has been reported on the evolution of the strength of ice during intervening "quiet" periods of low to no loading. Thus, it remains unknown if the mechanical properties of ice change during "quiet" periods. To address this question, we conducted a

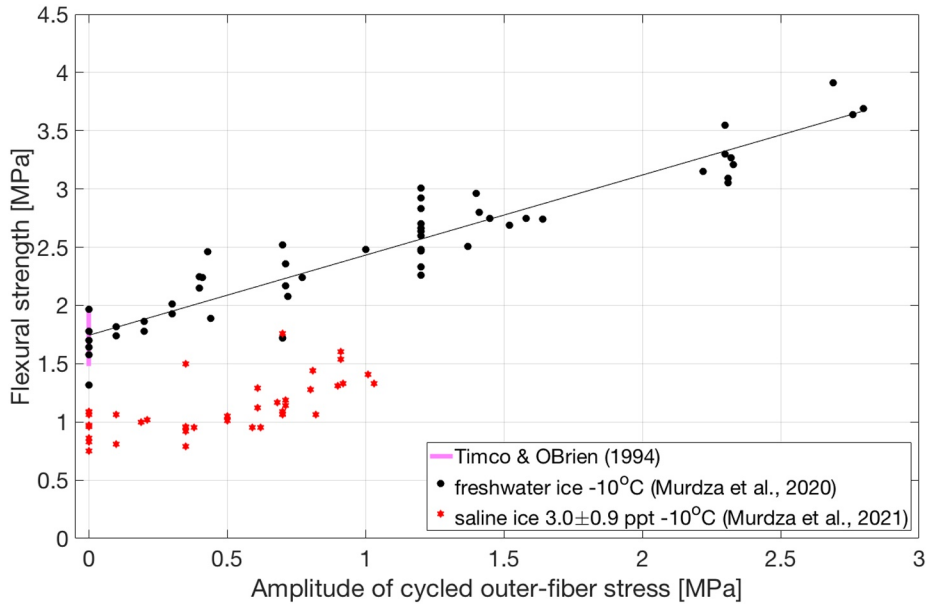

Figure 1. Flexural strength of freshwater and saline ice at −10°C as a function of reverse-cycled stress amplitude upon cycling at 1.4×10^{-4} s^{-1} outer-fiber strain rate. The solid pink line indicates the average flexural strength of non-cycled ice plus and minus one standard deviation (Timco & O'Brien, 1994).

series of experiments in which beams of both freshwater and saline ice were subjected to cyclic loading and then unloaded and allowed to anneal after which flexural strength was measured.

Early evidence of sea ice weakening under wave-driven in situ cyclic loading of sea ice beams was discussed by (Haskell et al., 1996; Langhorne et al., 1998), while recent studies on laboratory-grown fresh and saline ice suggested an increase in strength under cyclic loading (Murdza et al., 2020, 2021). The difference may be related to the thermo-mechanical history of natural sea ice that induces defects and flaws and to the absence of such history in laboratory-prepared specimens.

We have suggested earlier (Murdza et al., 2020) that the increase in flexural strength upon cyclic loading reflects the development of internal back stress, σ_b, that acts against the applied stress and that the back stress originates possibly from dislocation pileups which have been observed to form in ice (Liu et al., 1992, 1993). For example, in recent papers (Iliescu et al., 2017; Murdza et al., 2020) we showed the flexural strength of columnar-grained freshwater ice. It can be increased by as much as a factor of two or more by flexing at frequencies from 0.03 to 2 Hz at temperatures from −25 to −10°C. Similarly, we showed that the flexural strength of saline ice can be increased by as much as a factor of ∼1.5 by cycling at frequencies from 0.1 to 0.3 Hz and a temperature of −10°C (Murdza et al., 2021). The ice possessed a crystallographic growth texture in which the individual c-axes were confined more or less to a plane perpendicular to the long axis of the grains, but randomly oriented in that plane; it was termed S2 ice after Michel and Ramseier (Michel & Ramseier, 1971). The material was loaded in a direction perpendicular to the long axis of the columns such that shear stress acting on the basal slip system of most grains and on the grain boundaries. Upon gradually increasing the amplitude of the cyclic stress to a pre-determined outer-fiber level, σ_a, and then cycling at that level for ∼300 or more times, the flexural strength of freshwater ice, σ_{fc}, increased linearly with stress amplitude, in accord with the relationship:

$$\sigma_{fc} = \sigma_{f0} + k\sigma_a, \tag{1}$$

where σ_{f0} denotes the flexural strength of non-cycled material and k is a constant. Figure 1 shows an example for freshwater ice cycled at −10°C at a constant outer-fiber strain rate of 1.4×10^{-4} s^{-1} ∼0.1 Hz, which is approximately the frequency of natural ocean swells (Collins et al., 2015), where $\sigma_{f0} = 1.75$ MPa and $k = 0.68$. Saline ice exhibits similar behavior when tested at the same temperature and rate (Figure 1). The flexural strength was related to the brittle tensile strength and then attributed to the nucleation and immediate propagation of the

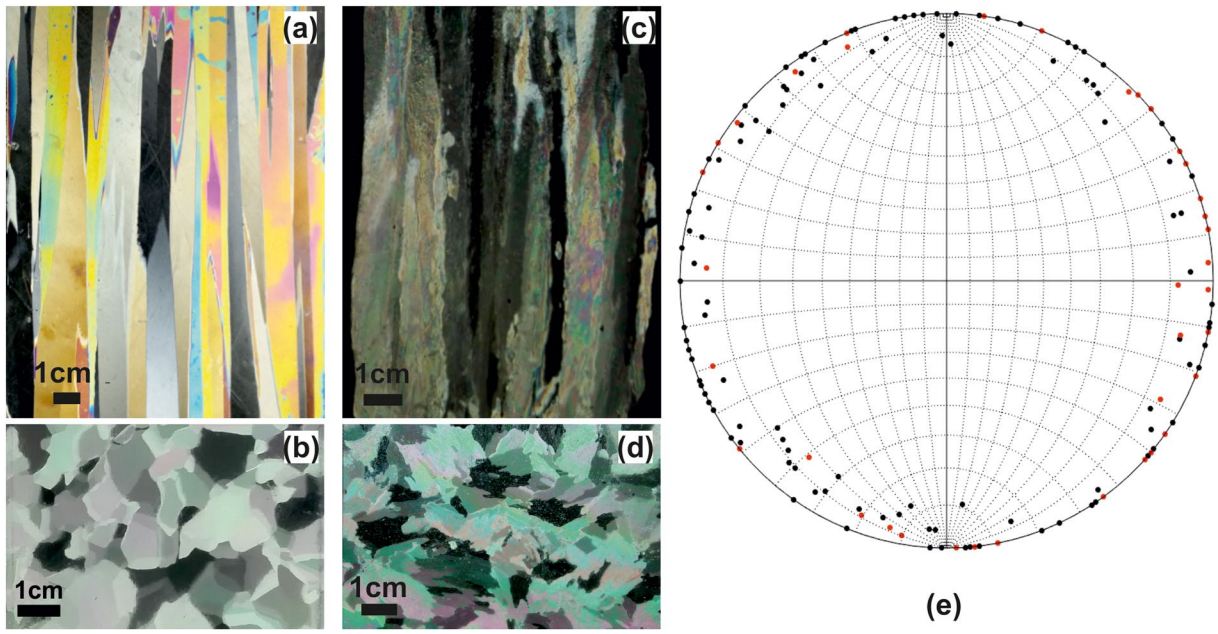

Figure 2. Photographs showing the microstructure of ice: vertical (a) and horizontal (b) thin sections of freshwater ice, vertical (c) and horizontal (d) thin sections of saline ice, and stereographic projection plot of crystal c-axis {0001} orientations for both freshwater (in black) and saline ice (in red) (e).

first crack, evident from the absence of remnant cracks of grain-size dimensions in the two parts of the broken specimens.

An implication of the suggestion that the increase in strength after cyclic loading is due to the development of back stress is that the back stress may be reduced and then eliminated upon annealing, restoring the ice strength to its non-cycled level. With that idea in mind, we performed new experiments and describe the results in this paper. Results show that annealing at a high homologous temperature for a sufficient amount of time does lead to a complete relaxation of the cyclically-induced strength of the ice. Moreover, we show that the sequence of strengthening and annealing is repeatable.

The obtained results, however, may not fully reflect natural phenomena due to some simplifications used in this work as compared to a real geophysical problem. For example, in addition to the absence of micro-cracks in our laboratory experiments, ice specimens had a constant temperature of −10 and −25°C, while ice covers in nature have temperature gradients with temperatures ranging from −1.8°C to, perhaps, as low as −40°C. Although our experiments describe well the ice behavior at intermediate temperatures, we think that as the temperature of the ice cover increases above −10°C and approaches the melting point, ice behavior may differ from the that described in this work. However, for the purpose of simply exposing for the first time the phenomenon of strength relaxation, we are proposing only a simplified physical model.

2. Materials and Methods

We studied the same kind of S2 freshwater and saline ice that we studied earlier (Iliescu et al., 2017; Murdza et al., 2018, 2019, 2020, 2021; Schulson et al., 2022), Figure 2. The material was produced in the laboratory by freezing both tap water and a solution containing 17.5 ± 0.2 ppt (parts per thousand) of salt mixture unidirectionally downward, following a standard procedure (Golding et al., 2014; Smith & Schulson, 1993). Of the ice so produced, thin-section analysis confirmed its S2 character, Figure 2e; its grain size (column diameter) was 5.5 ± 1.3 mm (freshwater ice) and 3.8 ± 0.9 mm (saline ice) and its density was 914.1 ± 1.6 kg·m^{-3} (freshwater ice) and 878 ± 11 kg·m^{-3} (saline ice). From such material, we machined beam-shaped specimens of dimensions $13 \times 75 \times 300$ mm^3 in which the long axis of the columnar grains was oriented perpendicular to the largest face. We prepared for testing 40 freshwater and 7 saline ice specimens.

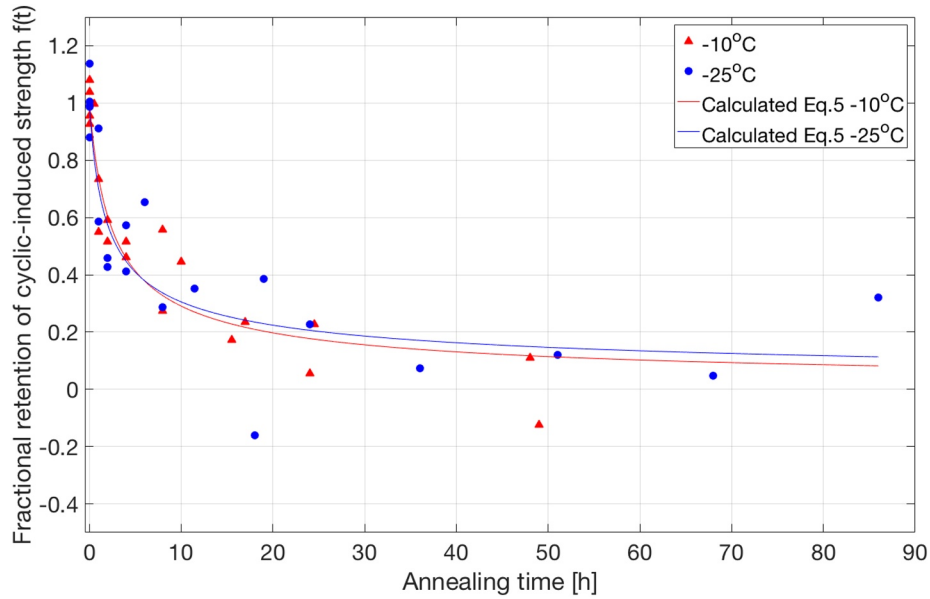

Figure 3. Fractional retention of cyclic-induced flexural strength of freshwater ice versus time at −25°C and −10°C. Points at $t = 0$ hr are associated with the strength of cycled ice before annealing. The ice had been flexed to outer-fiber stress of 2.3 MPa.

Flexural cycling and annealing were performed as follows: to impart an increase in strength prior to annealing, the ice was flexed in a fully reversed manner under 4-point loading under a constant outer-fiber center-point strain rate of 1.4×10^{-4} s^{-1}. The outer-fiber stress amplitude was gradually increased, as described earlier (Iliescu et al., 2017; Murdza et al., 2020, 2021), to a pre-determined level of either 0.7, 2.3, 2.5, or 2.7 MPa for freshwater ice and 0.9 MPa for saline ice, and then held constant at that level while the ice was cycled for an additional number of cycles, typically ∼300, until its strength saturated (see Figure 4 of Murdza et al. [2020]). Subsequently, the material was unloaded, allowed to anneal for up to 88 hr at the same temperature at which it was cycled, and then reloaded to failure without further cycling. In a few cases for freshwater ice, the sequence of strengthening-cum-annealing before bending to failure was repeated. All experiments were performed in a cold room at a constant temperature of either −25 or −10°C to which the ice was equilibrated. The flexural strength σ_f was calculated from the relationship under monotonic flexural loading:

$$\sigma_f = \frac{3PL}{4bh^2}, \tag{2}$$

where P is the applied load at rupture, $L = 254$ mm is the distance between the outer-pair of load lines and b and h denote width and thickness of the beam, respectively. Given that specimens were flexed in a reversed manner, no permanent macroscopic deformation of samples was observed after cycling, although microscopic local heterogeneous deformations might have occurred (Castelnau et al., 2008; Grennerat et al., 2012; Suquet et al., 2012). Therefore, during annealing, there was no macroscopic strain relaxation, unlike stress relaxation which is discussed below.

3. Results

3.1. Relaxation of Cyclic-Induced Strength

Figure 3 shows the first set of results. Before annealing, the freshwater ice was flexed to an outer-fiber stress of 2.3 MPa for ∼300 cycles after gradually raising the stress amplitude. That treatment raised the flexural strength at −25°C to $\sigma_{fc} = 3.4 \pm 0.14$ MPa from $\sigma_{f0} = 1.89 \pm 0.01$ MPa for non-cycled ice and at −10°C to $\sigma_{fc} = 3.2 \pm 0.1$ MPa from $\sigma_{f0} = 1.67 \pm 0.22$ MPa (Murdza et al., 2020). The figure plots, versus annealing time, the fractional retained strength, *f(t),* defined as:

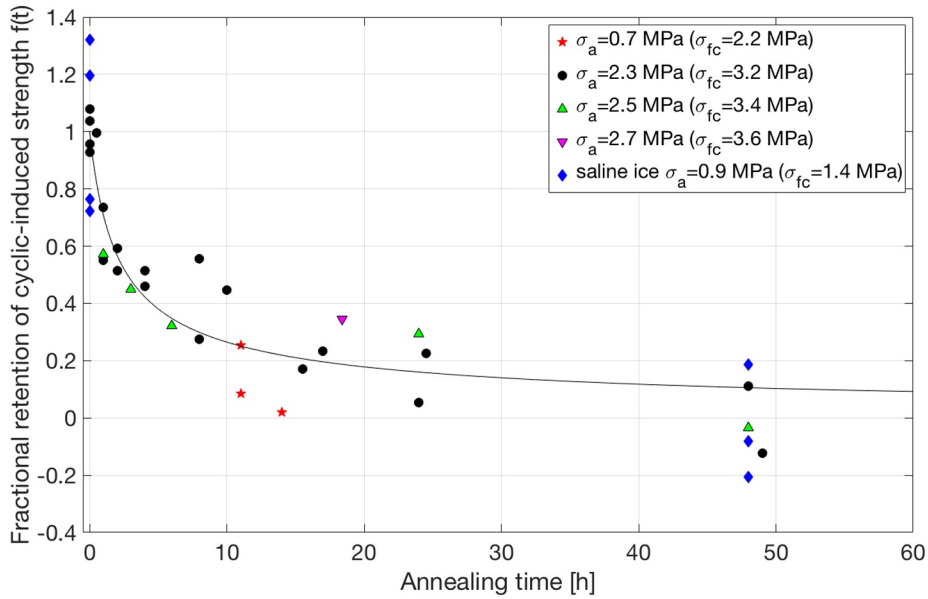

Figure 4. Fractional retention of cyclic-induced flexural strength of freshwater and saline ice versus annealing time at −10°C for ice that had been cycled at five different stress amplitudes, 0.7, 2.3, 2.5, 2.7 MPa (freshwater ice), and 0.9 MPa (saline ice), prior to annealing.

$$f(t) = \frac{\sigma_{fa}(t) - \sigma_{f0}}{\sigma_{fc} - \sigma_{f0}}, \tag{3}$$

where $\sigma_{fa}(t)$ denotes the flexural strength after annealing for time t. The numerator of Equation 3 denotes the back stress, σ_b, mentioned above, and the denominator denotes the increase in strength, $k\sigma_a$, that was imparted by cycling prior to annealing; that is,:

$$f(t) = \frac{\sigma_b}{k\sigma_a}. \tag{4}$$

The curves through the data in Figure 3 are the best fit lines determined through least-squares analysis ($R^2 = 0.95$ and standard error of the regression S is ∼0.15); the underlying functionality is discussed below. The results show that, for both temperatures, the flexural strength decreased rapidly during the first few hours of annealing and then continued to decrease with increasing time, returning to the level of the virgin, non-cycled material after about 2 to 3 days. It appears that the microstructural features that account for cyclic strengthening can be annihilated, similarly to the annihilation of dislocations during aging in ice single crystals (Taupin et al., 2008).

Figure 4 shows additional results for different levels of stress amplitude during cyclic strengthening. This figure shows the effect of annealing on the fractional retained strength of the material that had been cyclically strengthened at −10°C under different stress amplitudes, from 0.7 to 2.7 MPa. Included for completeness are the data shown in Figure 3. Again, relaxation occurred relatively quickly at first, and then more slowly, and the flexural strength approached the level of the virgin, non-cycled material after about 2 days. Within the scatter in the results, the rate of relaxation appears not to be affected by the initial strength σ_{fc} (given in the key to Figure 4) of the cycled material.

Figure 4 also provides results obtained from experiments conducted on saline ice. In these experiments, before annealing, the saline ice was flexed at −10°C to outer-fiber stress of 0.9 MPa for ∼300 cycles after gradually raising the stress amplitude, which raised the flexural strength to $\sigma_{fc} = 1.4 \pm 0.2$ MPa from $\sigma_{f0} = 0.96 \pm 0.13$ MPa (Murdza et al., 2021). These experiments demonstrated that the cyclically-induced flexural strength of saline ice is also fully relaxed.

In the experiments described above, the ice was subjected to a single strengthening-cum-annealing sequence before being bent to failure. In other experiments, the material was subjected to two such sequences. Specifically,

the freshwater ice was first strengthened by cycling ~300 times at −10°C at the same strain rate at a stress amplitude of $\sigma_a = 2.3$ MPa. It was then unloaded and annealed for ~48 hr at the same temperature, strengthened again by cycling under the same conditions, annealed again for the same time, and then strengthened for a third time in the same manner before being bent to failure. The final strength was 3.1 ± 0.1 MPa. This value is indistinguishable from the strength imparted after the first cycling, that is, 3.2 ± 0.1 MPa. In other words, it appears as though the microstructural features that account for cyclic strengthening and then for its relaxation can be created (during cycling) and then annihilated (during annealing) more than once.

We did not detect, using optical microscopy, recrystallized grains within thin sections that were prepared from specimens after cycling and from fully relaxed specimens, at least grains detectable at the level of resolution (~100 μm). The strain amplitude during cycling in the present experiments varied from $\sim 1 \times 10^{-4}$ to $\sim 5 \times 10^{-4}$ which is low compared to the standard 1% to reach the minimum creep rate after which recrystallization is typically observed (Budd & Jacka, 1989; Duval, 1981; Duval et al., 1983). The absence of new grains implies that a process other than recrystallization underlies the strengthening and relaxation (more below). We also did not detect remnant microcracks at the resolution of ~0.1 mm in the two parts of the ice beams that were obtained after breaking.

3.2. Analysis of Relaxation Kinetics

We modeled relaxation kinetics in terms of creep-controlled stress relaxation, Appendix 1. We imagined, as in the case of stress relaxation experiments, that over time elastic strain transforms to plastic strain through creep. Accordingly, upon invoking a power-law relationship, we found that the internal back stress, σ_b, to which we attribute cyclic-induced strengthening, decreases with time, t, according to the relationship:

$$\sigma_b(t) = \left(\frac{1}{(n-1) E B_0 t \ \exp\left(-\frac{Q}{RT}\right) + \frac{1}{\sigma_0^{n-1}}} \right)^{\frac{1}{n-1}}, \tag{5}$$

where $\sigma_0 = k\sigma_a$ denotes the back stress after cyclic strengthening at the onset of relaxation (at $t = 0$), E is Young's modulus, B is a temperature-dependent material constant described by $B = B_0 exp\left(-\frac{Q}{RT}\right)$, where Q is the activation energy, R is the universal gas constant, T is the absolute temperature, n is a material variable, and B_0 is another material constant. This relationship, normalized by σ_0, is shown by the curves through the data in Figure 3, using the derived parametric values for B and n (at $T = -10$°C: $n = 2.7$, $B = 4 \times 10^{-25}$ Pa^{-n} s^{-1}; at $T = -25$°C: $n = 2.9$, $B = 2.4 \times 10^{-26}$ Pa^{-n} s^{-1}) and by setting Young's modulus E to be 9.52 GPa (Snyder et al., 2016). Both the n-values and the B-values that we obtained are similar to values derived from creep experiments on ice (Barnes et al., 1971; Glen, 1955; Hobbs, 1974; Mellor & Smith, 1967; Nye, 1953). Assuming that B_0 is independent of temperature, we obtained values for the activation energy to be $Q = 101$ kJ mol^{-1} and for $B_0 = 5.7 \times 10^{-5}$ $Pa^{-n}\ s^{-1}$. Though we used a different approach, the obtained activation energy Q is consistent with the values that have been obtained for creep of ice (Barnes et al., 1971; Glen, 1955; Hobbs, 1974; Mellor & Smith, 1967; Nye, 1953; Steinemann, 1958), where n varies from ~2.5 to ~3.5 and Q varies from ~50 to ~150 kJ mol^{-1}.

4. Discussion

From the results shown above, the idea that motivated this work, namely that cyclic-induced strengthening may be relaxed, has been shown to be correct. The question then concerns the relaxation mechanism.

Firstly, we note that our measurements (Figure 3) did not reveal an effect of temperature. However, we do think that the temperature is a factor, particularly in saltwater ice as the temperature reaches the melting point. Rather, given the scatter in the data, and given the relatively small range of temperatures explored, an effect could not be unambiguously discerned. Most probably, the relaxation mechanism is thermally activated and, as a result, is expected to occur more slowly as the temperature is decreased.

On the mechanism itself, we cannot be definitive. However, given the fact that dislocations have been observed from in-situ creep experiments examined by synchrotron radiation (Liu et al., 1992, 1993) to pile up at grain boundaries, and given that pileups are expected to create back-stress against dislocation sources, a possible

candidate is dislocation climb. Climbing out of pileups will reduce the back stress on the dislocation source, thereby aiding relaxation. The fact that the activation energy deduced from the present experiments (Figures 3 and 4) is consistent with the value deduced from creep tests where the climb is a possible rate-controlling mechanism (Duval et al., 1983; Weertman, 1963) supports this possibility. Other more complex internal sub-structures associated with the isotropic component of hardening such as polarized dislocation substructure might also develop (Duval et al., 1983) followed by annihilation (Taupin et al., 2008), however, we refrain from further speculations. Neither recrystallization nor cracking (cracking detection performed through acoustic emission measurements over the frequency response of 3 kHz–3 MHz and minimum AE amplitude detection threshold of 45 dB by attaching the sensor to the ice surface, similar to Cole and Dempsey (2006); Langhorne and Haskell (1996); Lishman et al. (2020) were observed during cycling and annealing.

We suggest that strengthening and subsequent relaxation is a manifestation of a dynamic competition between the buildup of internal back stress and stress relaxation. Consistent with this view is the increase (Murdza et al., 2020), albeit a small one, in the measured flexural strength upon increasing the frequency of cycling.

Although our observations were generated from a study of columnar-grained ice, we think the relaxation is not limited to that form of the material. There is evidence, for instance, that granular ice (equiaxed and randomly oriented aggregates) exhibits cyclic strengthening under direct tensile-compressive loading (D. M. Cole, 1990). In addition, strengthening of columnar-grained S2 ice has been observed earlier (Gupta et al., 1998; Iliescu & Schulson, 2002) where the ice was cyclically loaded across-column in compression. We expect that in the above cases, too, the ice will relax.

The obtained results in the present study indicate that the ice with no thermo-mechanical history and no microcracks is the weakest and, thus, most susceptible to flexural failure after long periods of annealing or the absence of ocean waves when internal stresses have fully relaxed. Once stresses in ice start to increase gradually, ice becomes stronger and less susceptible to failure. Although these results have an impact on the understanding of the role of ocean waves on sea ice covers, and particularly on its fragmentation, we think that other factors that are not considered in this work may play an important role and affect ice behavior. For example, thinning of the ice, presence of microcracks, and other flaws as a result of thermo-mechanical history and temperatures near melting point may change the ice behavior dramatically, for example, weakening under the action of ocean waves as described earlier (Haskell et al., 1996; Langhorne et al., 1998).

5. Conclusions

From new, systematic experiments on the flexural strength of S2 columnar-grained freshwater and saline ice without thermo-mechanical history and microcracks stressed principally across the columns through reversed cyclic loading and following annealing at temperatures of −25°C and −10°C, it is concluded that:

1. Ice strength imparted through cyclic loading is fully relaxed upon annealing in both freshwater and saline ice in about 2 days at both −25°C and −10°C.
2. Ice can be strengthened multiple times to the same value of strength if allowed to anneal after each loading.
3. Relaxation of the flexural strength during annealing is due to the relaxation of cyclically-induced internal back stress.
4. Strengthening and subsequent relaxation are attributed to a dynamic competition between the buildup of internal back stress and a process of creep-driven stress relaxation.

Appendix: Internal Back-Stress Relaxation

The idea about stress relaxation can be summarized as follows: we imagine that within the grains of the cyclically-strengthened ice the total strain at any moment can be viewed as the sum of elastic ε_e and plastic ε_p strains anelastic strain is neglected as it is only ∼5% of elastic strain (Murdza et al., 2018). During relaxation, the reduction of internal stress is due to the gradual reduction of the elastic deformation and the increase of the plastic deformation by the same value. For simplicity, we neglect anelastic strain ε_{an}.

From the theory of elasticity, that is, $\varepsilon_e = {}^{\sigma_b}/_{E}$, and from power-law creep, that is, $\dot{\varepsilon}_p = B\sigma_b^n$, we obtain the relationship:

$$\frac{d\sigma_b}{dt} = -EB_0\sigma_b^n \exp\left(-\frac{Q}{RT}\right), \tag{A1}$$

where σ_b is the back stress, E is Young's modulus and B is a temperature-dependent material constant described by $B = B_0 exp\left(-\frac{Q}{RT}\right)$, where Q is the activation energy, R is the universal gas constant, T is the absolute temperature, n is a material variable, and B_0 is another material constant. Integration of Equation A1 results in the relationship:

$$\sigma_b(t) = \left(\frac{1}{\left((n-1)EB_0 t \exp\left(-\frac{Q}{RT}\right) + \frac{1}{\sigma_0^{n-1}}\right)}\right)^{\frac{1}{n-1}} \tag{A2}$$

where σ_0 is the level of back stress at the onset of annealing ($t = 0$).

Procedure for derivation of Q, B, B_0 and n values:

1. Based on the fit described in the text (using the least square method) the values for B and n at -25°C and -10°C were determined
2. After that, it was assumed that B_0 is independent of temperature
3. The following two equations were obtained: (1) $B_1 = B_0 \exp(^{-Q}/_{RT_1})$; 2) $B_2 = B_0 \exp(^{-Q}/_{RT_2})$, where B_1 and B_2 are the values of B for temperatures of -25°C and -10°C, respectively

By solving the system of two equations, B_0 and Q were determined.

Data Availability Statement

The data used in this research can be accessed at https://doi.org/10.18739/A20G3H029.

Acknowledgments
We acknowledge helpful discussions with Harold Frost, Robert Gagnon, and Daniel Iliescu. This work was supported by the US Department of the Interior-Bureau of Safety and Environmental Enforcement, contract no. E16PC00005 and by National Science Foundation (FAIN 1947-107).

References

Ardhuin, F., Otero, M., Merrifield, S., Grouazel, A., & Terrill, E. (2020). Ice breakup controls dissipation of wind waves across Southern ocean sea ice. *Geophysical Research Letters*, *47*(13). https://doi.org/10.1029/2020gl087699

Asplin, M. G., Galley, R., Barber, D. G., & Prinsenberg, S. (2012). Fracture of summer perennial sea ice by ocean swell as a result of Arctic storms. *Journal of Geophysical Research: Oceans*, *117*(6), 1–12. https://doi.org/10.1029/2011jc007221

Barnes, P., Tabor, D., & Walker, J. C. F. (1971). The friction and creep of polycrystalline ice. *Proceedings of the Royal Society A: Mathematical, Physical & Engineering Sciences*, *324*(1557), 127–155. https://doi.org/10.1098/rspa.1971.0132

Budd, W. F., & Jacka, T. H. (1989). A review of ice rheology for ice sheet modelling. *Cold Regions Science and Technology*, *16*(2), 107–144. https://doi.org/10.1016/0165-232x(89)90014-1

Burns, J. A., & Matthews, M. S. (1986). *Satellites* (Vol. 77). University of Arizona Press.

Castelnau, O., Duval, P., Montagnat, M., & Brenner, R. (2008). Elastoviscoplastic micromechanical modeling of the transient creep of ice. *Journal of Geophysical Research*, *113*(B11), B11203. https://doi.org/10.1029/2008jb005751

Cole, D., & Dempsey, J. (2006). Laboratory observations of acoustic emissions from Antarctic first-year sea ice cores under cyclic loading. In *18th International POAC Conference* (p. Vol 3, 1083–1092).

Cole, D. M. (1990). Reversed direct-stress testing of ice: Initial experimental results and analysis. *Cold Regions Science and Technology*, *18*(3), 303–321. https://doi.org/10.1016/0165-232x(90)90027-t

Collins, C. O., Rogers, W. E., Marchenko, A., & Babanin, A. V. (2015). In situ measurements of an energetic wave event in the Arctic marginal ice zone. *Geophysical Research Letters*, *42*(6), 1863–1870. https://doi.org/10.1002/2015gl063063

Duval, P. (1981). Creep and fabrics of polycrystalline ice under shear and compression. *Journal of Glaciology*, *27*(95), 129–140. https://doi.org/10.3189/s002214300001128x

Duval, P., Ashby, M. F., & Anderman, I. (1983). Rate-controlling processes in the creep of polycrystalline ice. *Journal of Physical Chemistry*, *87*, 4066–4074. https://doi.org/10.1021/j100244a014

Francis, O. P., Panteleev, G. G., & Atkinson, D. E. (2011). Ocean wave conditions in the Chukchi Sea from satellite and *in situ* observations. *Geophysical Research Letters*, *38*(24), L24610https://doi.org/10.1029/2011gl049839

Glen, J. W. (1955). The creep of polycrystalline ice. *Proceeding of the Royal Society of London Series A. Mathematical and Physical Sciences*, *228*(1175), 519–538. https://doi.org/10.1098/rspa.1955.0066

Golding, N., Snyder, S. A., Schulson, E. M., & Renshaw, C. E. (2014). Plastic faulting in saltwater ice. *Journal of Glaciology*, *60*(221), 447–452. https://doi.org/10.3189/2014jog13j178

Grennerat, F., Montagnat, M., Castelnau, O., Vacher, P., Moulinec, H., Suquet, P., & Duval, P. (2012). Experimental characterization of the intragranular strain field in columnar ice during transient creep. *Acta Materialia*, *60*(8), 3655–3666. https://doi.org/10.1016/j.actamat.2012.03.025

Gupta, V., Bergström, J., & Picu, C. R. (1998). Effect of step-loading history and related grain-boundary fatigue in freshwater columnar ice in the brittle deformation regime. *Philosophical Magazine Letters*, *77*(5), 241–247.

Hammond, N. P., Barr, A. C., Cooper, R. F., Caswell, T. E., & Hirth, G. (2018). Experimental constraints on the fatigue of icy satellite lithospheres by tidal forces. *Journal of Geophysical Research: Planets*, *123*(2), 390–404. https://doi.org/10.1002/2017je005464

Haskell, T. G., Robinson, W. H., & Langhorne, P. J. (1996). Preliminary results from fatigue tests on in situ sea ice beams. *Cold Regions Science and Technology*, *24*(2), 167–176. https://doi.org/10.1016/0165-232x(95)00015-4

Hobbs, P. V. (1974). *Ice Physics*. Clarendon.

Holdsworth, G. (1969). Flexure of a floating ice tongue. *Journal of Glaciology*, *8*(54), 385–397. https://doi.org/10.1017/s0022143000026976

Iliescu, D., Murdza, A., Schulson, E. M., & Renshaw, C. E. (2017). Strengthening ice through cyclic loading. *Journal of Glaciology*, *63*(240), 663–669. https://doi.org/10.1017/jog.2017.32

Iliescu, D., & Schulson, E. M. (2002). Brittle compressive failure of ice: Monotonic versus cyclic loading. *Acta Materialia*, *50*(8), 2163–2172. https://doi.org/10.1016/s1359-6454(02)00060-5

Kohout, A. L., Williams, M. J. M., Dean, S. M., & Meylan, M. H. (2014). Storm-induced sea-ice breakup and the implications for ice extent. *Nature*, *509*(7502), 604–607. https://doi.org/10.1038/nature13262

Kohout, A. L., Williams, M. J. M., Toyota, T., Lieser, J., & Hutchings, J. (2016). In situ observations of wave-induced sea ice breakup. *Deep-Sea Research Part II Topical Studies in Oceanography*, *131*, 22–27. https://doi.org/10.1016/j.dsr2.2015.06.010

Langhorne, P. J., & Haskell, T. G. (1996). Acoustic emission during fatigue experiments on first year sea ice. *Cold Regions Science and Technology*, *24*(3), 237–250. https://doi.org/10.1016/0165-232x(95)00021-3

Langhorne, P. J., Squire, V. A., Fox, C., & Haskell, T. G. (1998). Break-up of sea ice by ocean waves. *Annals of Glaciology*, *27*, 438–442. https://doi.org/10.3189/s0260305500017869

Lishman, B., Marchenko, A., Sammonds, P., & Murdza, A. (2020). Acoustic emissions from in situ compression and indentation experiments on sea ice. *Cold Regions Science and Technology*, *172*, 102987. https://doi.org/10.1016/j.coldregions.2019.102987

Liu, A. K., Mollo-Christensen, E., Liu, A. K., & Mollo-Christensen, E. (1988). Wave propagation in a solid ice pack. *Journal of Physical Oceanography*, *18*, 1702–1712. https://doi.org/10.1175/1520-0485(1988)018<1702:wpiasi>2.0.co;2

Liu, F., Baker, I., & Dudley, M. (1993). Dynamic observations of dislocation generation at grain boundaries in ice. *Philosophical Magazine A: Physics of Condensed Matter, Structure, Defects and Mechanical Properties*, *67*(5), 1261–1276. https://doi.org/10.1080/01418619308224770

Liu, F., Baker, I., Yao, G., & Dudley, M. (1992). Dynamic observation of dislocation sources at grain boundaries in ice. *Philosophical Magazine Letters*, *65*(5), 279–281. https://doi.org/10.1080/09500839208207548

Massom, R. A., & Stammerjohn, S. E. (2010). Antarctic sea ice change and variability - physical and ecological implications. *Polar Science*, *4*(2), 149–186. https://doi.org/10.1016/j.polar.2010.05.001

Mellor, M., & Smith, J. H. (1967). Creep of snow and ice. In *Physics of snow and ice* (pp. 843–855).

Meylan, M. H., Bennetts, L. G., Cavaliere, C., Alberello, A., & Toffoli, A.(2015). Experimental and theoretical models of wave-induced flexure of a sea ice floe. *Physics of Fluids*, *27*(4), 041704. https://doi.org/10.1063/1.4916573

Meylan, M. H., Bennetts, L. G., & Kohout, A. L. (2014). In situ measurements and analysis of ocean waves in the Antarctic marginal ice zone. *Geophysical Research Letters*, *41*(14), 5046–5051. https://doi.org/10.1002/2014gl060809

Michel, B., & Ramseier, R. O. (1971). Classification of river and lake ice. *Canadian Geotechnical Journal*, *8*(1), 36–45. https://doi.org/10.1139/t71-004

Murdza, A., Marchenko, A., Schulson, E. M., Renshaw, C., Sakharov, A., Karulin, E., & Chistyakov, P. (2020). Results of preliminary cyclic loading experiments on natural lake ice and sea ice. In *25th IAHR International Symposium on ice* (pp. 1–10).

Murdza, A., Marchenko, A., Schulson, E. M., & Renshaw, C. E. (2021). Cyclic strengthening of lake ice. *Journal of Glaciology*, *67*(261), 182–185. https://doi.org/10.1017/jog.2020.86

Murdza, A., Polojärvi, A., Schulson, E. M., & Renshaw, C. E. (2021). The flexural strength of bonded ice. *The Cryosphere*, *15*, 2957–2967. https://doi.org/10.5194/tc-15-2957-2021

Murdza, A., Schulson, E. M., & Renshaw, C. E. (2018). Hysteretic behavior of freshwater ice under cyclic loading : Preliminary results. In *24th IAHR International Symposium on ice* (pp. 185–192).

Murdza, A., Schulson, E. M., & Renshaw, C. E. (2019). The effect of cyclic loading on the flexural strength of columnar freshwater ice. In *Proceedings of the International conference on Port and ocean Engineering under Arctic conditions*, POAC (Vol. 2019-June).

Murdza, A., Schulson, E. M., & Renshaw, C. E. (2020). Strengthening of columnar-grained freshwater ice through cyclic flexural loading. *Journal of Glaciology*, *66*(258), 556–566. https://doi.org/10.1017/jog.2020.31

Murdza, A., Schulson, E. M., & Renshaw, C. E. (2021). Behavior of saline ice under cyclic flexural loading. *The Cryosphere*, *15*, 2415–2428. https://doi.org/10.5194/tc-15-2415-2021

Nye, J. F. (1953). The flow law of ice from measurements in glacier tunnels, laboratory experiments and the Jungfraufirn borehole experiment. *Proceedings of the Royal Society of London - Series A: Mathematical and Physical Sciences*, *219*(1139), 477–489.

Pistone, K., Eisenman, I., & Ramanathan, V. (2014). Observational determination of albedo decrease caused by vanishing Arctic sea ice. *Proceedings of the National Academy of Sciences of the United States of America*, *111*(9), 3322–3326. https://doi.org/10.1073/pnas.1318201111

Prinsenberg, S. J., & Peterson, I. K. (2011). Observing regional-scale pack-ice decay processes with helicopter-borne sensors and moored upward-looking sonars. *Annals of Glaciology*, *52*(57), 35–42. https://doi.org/10.3189/172756411795931688

Richter-Menge, J. A., McNutt, S. L., Overland, J. E., & Kwok, R. (2002). Relating arctic pack ice stress and deformation under winter conditions. *Journal of Geophysical Research: Oceans*, *107*(10), SHE15-1–SHE15-13. https://doi.org/10.1029/2000jc000477

Schulson, E. M., Murdza, A., & Renshaw, C. E. (2022). Mechanisms of cyclic strengthening and Recovery of polycrystalline ice. In J.Tuhkuri, & A.Polojärvi (Eds.), *IUTAM Symposium on Physics and Mechanics of sea ice. IUTAM Bookseries* (Vol. 39). Springer. https://doi.org/10.1007/978-3-030-80439-8_1

Sergienko, O. V. (2010). Elastic response of floating glacier ice to impact of long-period ocean waves. *Journal of Geophysical Research*, *115*(F4), F04028. https://doi.org/10.1029/2010jf001721

Smith, T. R., & Schulson, E. M.(1993). The brittle compressive failure of fresh-water columnar ice under biaxial loading. *Acta Metallurgica et Materialia*, *41*(1), 153–163. https://doi.org/10.1016/0956-7151(93)90347-u

Snyder, S. A., Schulson, E. M., & Renshaw, C. E. (2016). Effects of prestrain on the ductile-to-brittle transition of ice. *Acta Materialia*, *108*, 110–127. https://doi.org/10.1016/j.actamat.2016.01.062

Steele, M. (1992). Sea ice melting and floe geometry in a simple ice-ocean model. *Journal of Geophysical Research*, *97*(C11), 17729–17738. https://doi.org/10.1029/92jc01755

Steinemann, S. (1958). Experim entelle untersuchungen zur plastizitat von Eis. Beitrage zur Geologie der Schweiz. *Hydrologie*no.*10*, 46–50.

Stopa, J. E., Sutherland, P., & Ardhuin, F. (2018). Strong and highly variable push of ocean waves on Southern Ocean sea ice. *Proceedings of the National Academy of Sciences of the United States of America*, *115*(23), 5861–5865. https://doi.org/10.1073/pnas.1802011115

Suquet, P., Moulinec, H., Castelnau, O., Montagnat, M., Lahellec, N., Grennerat, F., et al. (2012). Multi-scale modeling of the mechanical behavior of polycrystalline ice under transient creep, Procedia IUTAM. In *Procedia IUTAM* (Vol. 3, pp. 76–90). Elsevier B.V. https://doi.org/10.1016/j.piutam.2012.03.006

Sutherland, P., & Dumont, D. (2018). Marginal ice zone thickness and extent due to wave radiation stress. *Journal of Physical Oceanography*, *48*(8), 1885–1901. https://doi.org/10.1175/jpo-d-17-0167.1

Taupin, V., Richeton, T., Chevy, J., Fressengeas, C., Weiss, J., Louchet, F., & Miguel, M. C. (2008). Rearrangement of dislocation structures in the aging of ice single crystals. *Acta Materialia*, *56*(7), 1555–1563. https://doi.org/10.1016/j.actamat.2007.12.011

Thomson, J., & Rogers, W. E. (2014). Swell and sea in the emerging Arctic Ocean. *Geophysical Research Letters*, *41*(9), 3136–3140. https://doi.org/10.1002/2014gl059983

Timco, G. W., & O'Brien, S. (1994). Flexural strength equation for sea ice. *Cold Regions Science and Technology*, *22*(3), 285–298. https://doi.org/10.1016/0165-232x(94)90006-x

Toffoli, A., Bennetts, L. G., Meylan, M. H., Cavaliere, C., Alberello, A., Elsnab, J., & Monty, J. P. (2015). Sea ice floes dissipate the energy of steep ocean waves. *Geophysical Research Letters*, *42*(20), 8547–8554. https://doi.org/10.1002/2015gl065937

Vinogradov, O. G., & Holdsworth, G. (1985). Oscillation of a floating glacier tongue. *Cold Regions Science and Technology*, *10*(3), 263–271. https://doi.org/10.1016/0165-232x(85)90037-0

Weertman, J. (1963). The Eshelby–Schoeck viscous dislocation damping mechanism applied to the steady-state creep of ice. In W. D. Kingery (Ed.), *Ice and snow; properties processes, and applications: Proceedings of a conference held at the Massachusetts Institute of Technology* (pp. 28–33). M.I.T. Press.

Zhang, R., Wang, H., Fu, Q., Rasch, P. J., & Wang, X. (2019). Unraveling driving forces explaining significant reduction in satellite-inferred Arctic surface albedo since the 1980s. *Proceedings of the National Academy of Sciences of the United States of America*, *116*(48), 23947–23953. https://doi.org/10.1073/pnas.1915258116